

## Supporting Information

### Measurements

#### 1. Water uptake and swelling ratio

In order to calculate the membrane water uptake and swelling ratio, the samples were soaked in DDI water at room temperature for 24 h. After water was removed from the membrane surface, the weight and dimension of the membranes were measured immediately. Then, the membranes were dried at 60 °C under vacuum until a constant weight and dimension were achieved. The water uptake (WU) and swelling ratio both in-plane (I-SR) and through-plane (T-SR) were calculated with the following equations:

$$WU(\%) = \frac{W_w - W_d}{W_d} \times 100$$

$$I - SR(\%) = \frac{S_w - S_d}{S_d} \times 100$$

$$T - SR(\%) = \frac{T_w - T_d}{T_d} \times 100$$

where  $W_w$  (g),  $S_w$  (mm<sup>2</sup>) and  $T_w$  (mm) are the weight, surface area and thickness of hydrated membranes, respectively.  $W_d$ ,  $S_d$  (mm<sup>2</sup>) and  $T_d$  (mm) are the weight, surface and thickness of dried membranes, respectively.

#### 2. Ionic conductivity

The hydroxide conductivities of membranes were measured using an AC impedance technique in the in-plane direction. The following equation was used to determine the ionic conductivity.

$$\sigma = \frac{L}{RA}$$

where  $\sigma$  denotes the ionic conductivity (S cm<sup>-1</sup>),  $L$  is the distance (cm) between the reference electrode and the working electrode,  $A$  is the cross-sectional area of the membrane (cm<sup>2</sup>), and  $R$  the measured resistance of the membrane ( $\Omega$ ).

#### 3. Activation energy

The dependence of the ionic conductivity of membranes on temperature was evaluated by the Arrhenius equation:

$$\sigma = A \exp\left(\frac{-E_a}{RT}\right)$$

where  $\sigma$  is the ionic conductivity (S cm<sup>-1</sup>),  $A$  is the pre-exponential factor (sec<sup>-1</sup>),  $E_a$  is activation energy (J mol<sup>-1</sup>),  $R$  is the universal gas constant (8.3144 J mol<sup>-1</sup> K<sup>-1</sup>) and  $T$  is the absolute temperature (K).

#### 4. Porosity

The porosity was measure by immersing the membranes in the isopropanol bath for 24 h. After that, the weight of saturated membranes was recorded. The porosity was determined according to the equation:

$$Porosity(\%) = \frac{(M_s - M_d)/\rho_i}{A \times t}$$

where  $M_s$  and  $M_d$  represent the weight of the saturated and dry membranes, respectively.  $\rho_i$  is the density of the isopropanol.  $A$  and  $t$  represent the surface area and thickness of the dry membrane, respectively.

##### 5. Calculations of specific capacity and energy density

The specific capacity ( $\text{mAh g}^{-1}$ ) was calculated according to the equation below:

$$\frac{\text{Current drain} \times \text{Discharge hours}}{\text{Weight of zinc electrode}}$$

The power density ( $\text{mW g}^{-1}$ ) was calculated according to the equation below:

$$\frac{\text{Current drain} \times \text{Discharge voltage}}{\text{Weight of zinc electrode}}$$

where the weight of zinc electrode is 40 mg.

## List of Figures

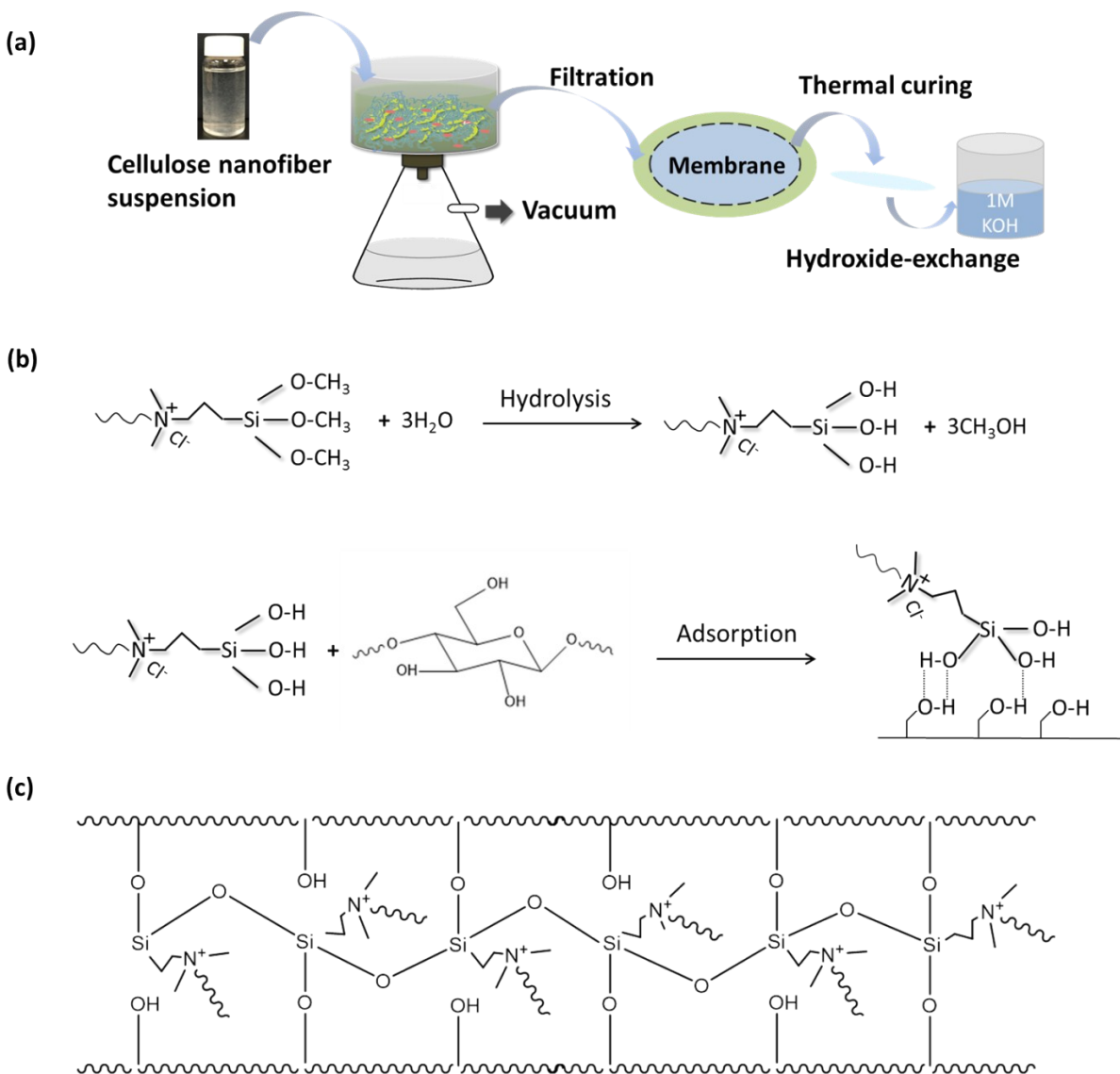


**Fig. S1** (a) The procedure for the preparation of the quaternary ammonia-functionalized nanocellulose (QAFC) membrane. (b) Proposed reaction mechanism for cellulose surface-functionalization with DMOAP. (c) The covalent cross-linking bonding-network of the QAFC membrane.

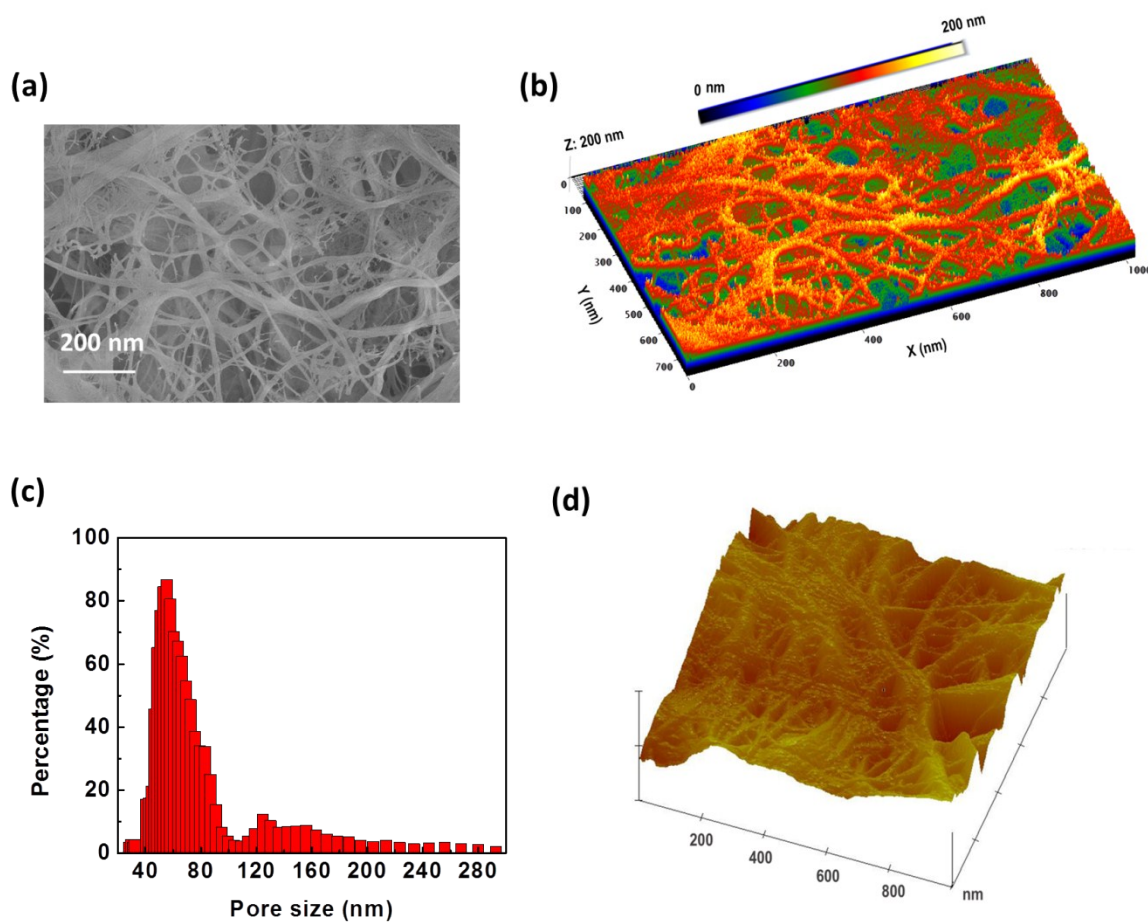


**Fig.S2** (a) SEM surface image of the 2-QAFC membrane and (b) corresponding three-dimensional surface morphology, showing its nanoporous structure up to a depth of 200 nm. (c) Pore size distributions of the 2-QAFC membrane obtained from AFM image analysis, and (d) corresponding three-dimensional AFM image.

An interconnected nanoporous structure of the 2-QAFC membrane was identified by SEM (Fig. S2a). Fig. S2b exhibits a three-dimensional, visualized image of the membrane surface morphology over an area of 1,000 × 780 nm with a depth of up to 200 nm. The color intensity shows the vertical profile of the membrane surface with the light regions being the highest points and the dark regions being pores and depressions. The pores are clearly visible as various well-defined green and blue regions of the image, having the pore size ranges from tens of nanometers to hundreds of nanometers. The pore size distributions (Fig. S2c) of the membrane obtained from AFM image (Fig. S2d) further place them clearly in the nanosized range. The pore size ranges from 25 ~ 300 nm. In addition, the porosity of the 2-QAFC membrane is measured to be 72.8%. The high porosity is deemed to account in part for the high water uptake and the resultant high ionic conductivity.

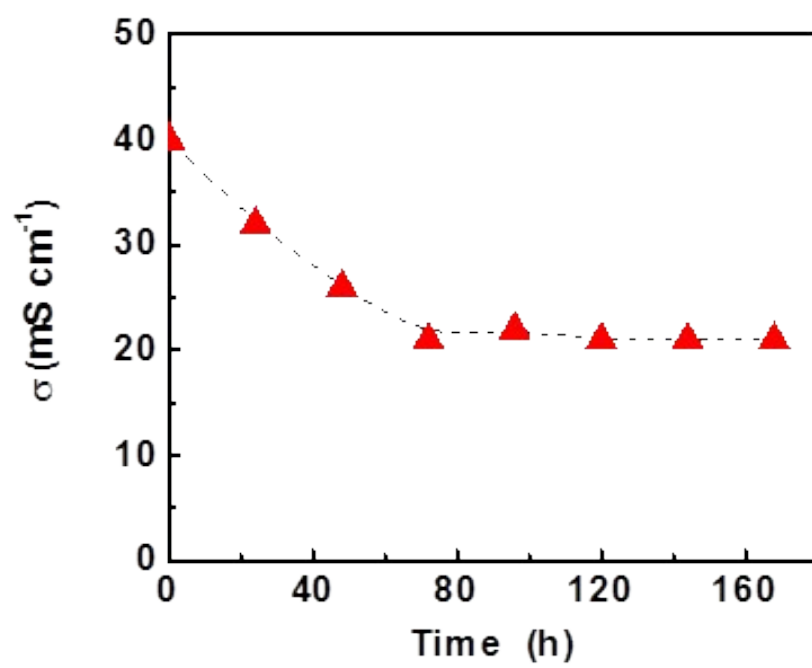


**Fig.S3** Ionic conductivity of the 2-QAFC membrane as a function of time.

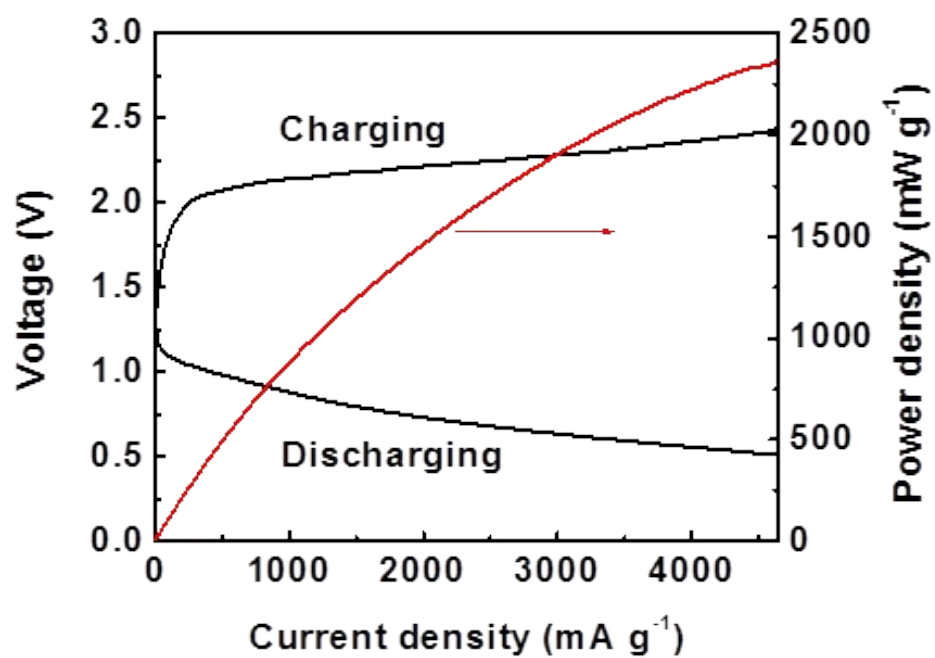


**Fig. S4** Charge and discharge polarization curves and corresponding power density plot of the battery using the 2-QAFC membrane.

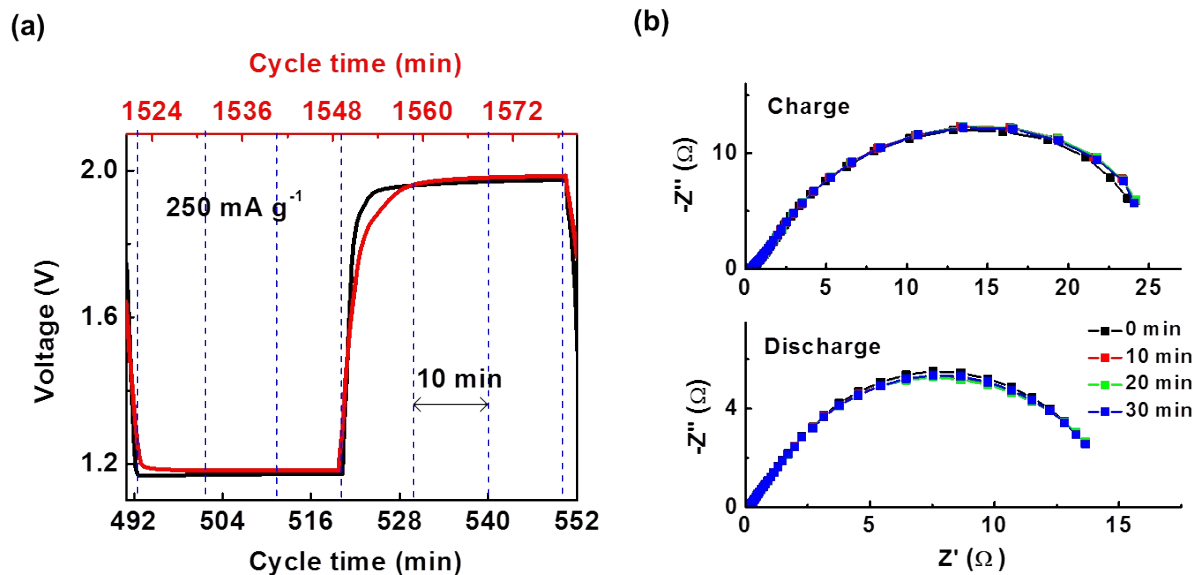


**Fig. S5** (a) The galvanostatic cycling plots of the 2-QAFC battery under a current density of 250 mA g<sup>-1</sup>, taken at two different 60 min-cycle segments and (b) corresponding EIS spectra at designated time intervals (10 min).

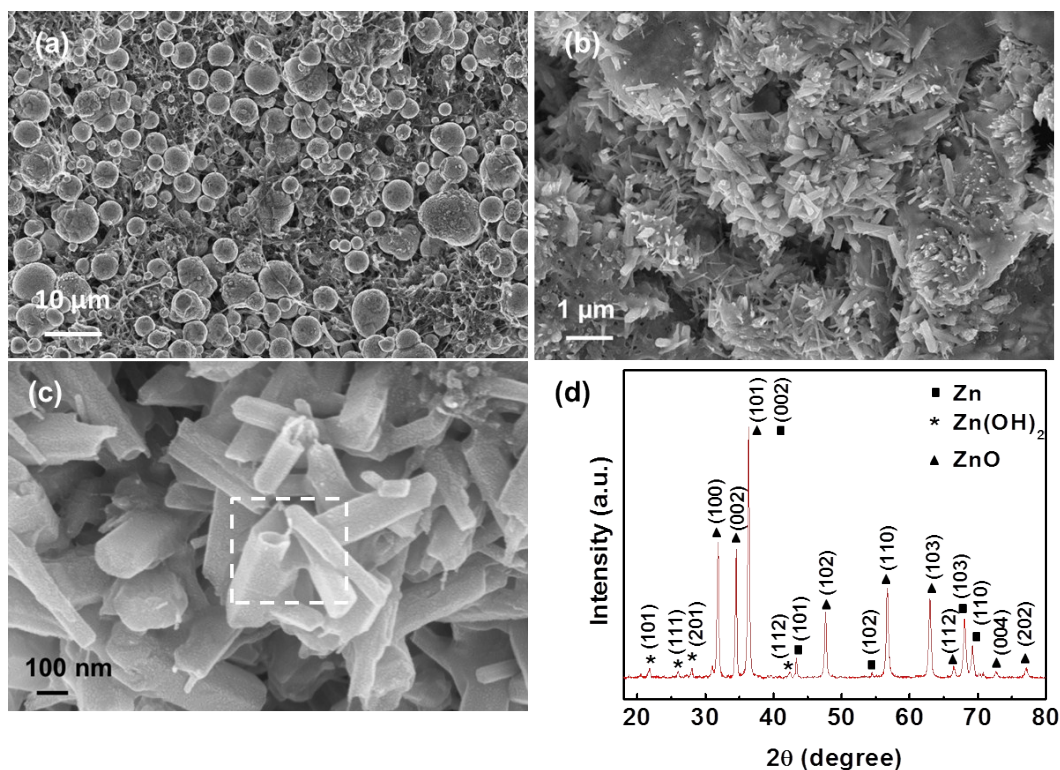


**Fig. S6** (a) fresh zinc electrode and (b) cycled zinc electrode (finished by discharge). (c) The high magnification SEM image of the square region of (b), outlined in white. (d) XRD pattern of the cycled zinc electrode. The battery using the 2-QAFC membrane was cycled at a current density of 250 mA g<sup>-1</sup> with a 60 min per cycle period.

SEM image of a zinc electrode prior to the cycling shows a porous structure in nature, where zinc particles are well-distributed (Fig. S6a). Fig. S6b exhibits the morphology of the cycled zinc electrode. It shows that hollow, rod-shaped nanograins, with an average diameter of ~100 nm and about ~1 μm in length, are partially deposited on the surface of zinc particles (Fig. S6c). This observation is contrary to the well-known compact passivation layer of zinc oxide species, which prevent direct contact of hydroxide ions with remaining active zinc species, indicative of a good reversibility of the zinc electrode. The cycled zinc electrode was further identified by XRD (Fig. S6d), containing zinc, zinc hydroxide and zinc oxide species (Zn (JCPDS 04-0831); Zn(OH)<sub>2</sub> (JCPDS 38-0385); ZnO (JCPDS 036-1451)).



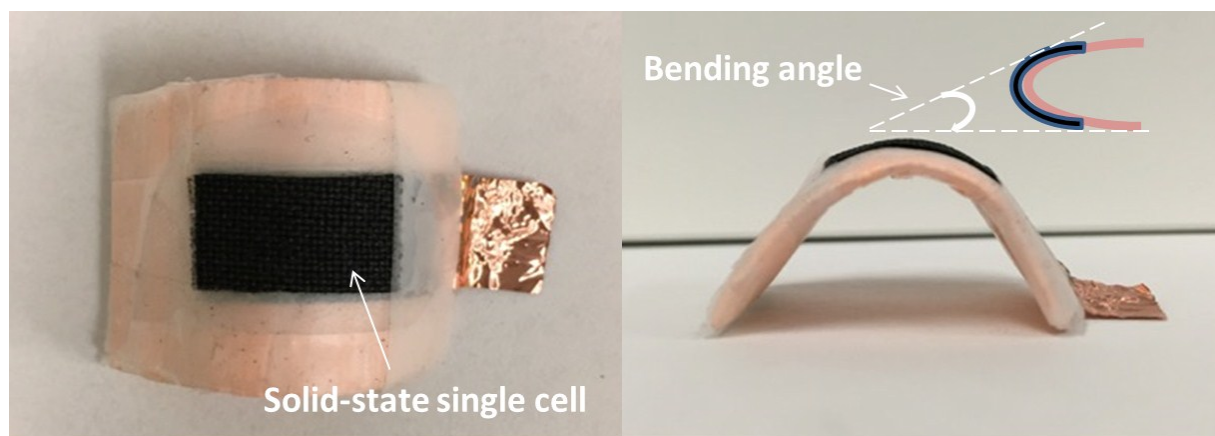


**Fig. S7** A photograph of a solid-state single zinc-air cell device under the bending condition.

**Table S1** Properties of the 2-QAFC membrane.

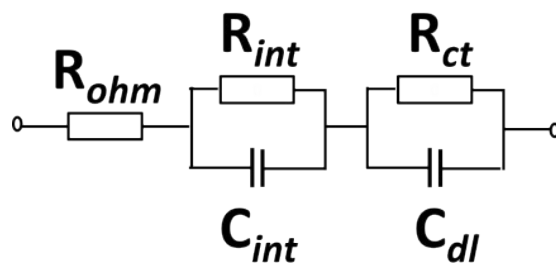
Anion type	Thickness [ $\mu\text{m}$ ]	Water uptake [%]	$\sigma$ [ $\text{mS cm}^{-1}$ ]
$\text{OH}^-$	30	96.5	21.2
$\text{CO}_3^{2-}$ <sup>a)</sup>	30	96.2	18.7

<sup>a)</sup> The membranes were exchanged to the  $\text{CO}_3^{2-}$  form by their immersion in a large excess of aqueous 1M  $\text{K}_2\text{CO}_3$ , and were thoroughly washed by water to remove the excess  $\text{K}_2\text{CO}_3$ .<sup>1</sup>

**Table S2** The values of the equivalent circuit <sup>d)</sup> elements based on the EIS analysis of the zinc-air battery.

Bending angle ( $^\circ$ )	$R_{\text{ohm}}$ <sup>a)</sup> (ohm)	$R_{\text{int}}$ <sup>b)</sup> (ohm)	$R_{\text{ct}}$ <sup>c)</sup> (ohm)
0	0.77	1.66	2.08
60	0.76	1.68	2.19
90	0.77	1.66	2.28
120	0.77	1.67	2.27

<sup>a)</sup> Ohmic resistance. <sup>b)</sup> Interfacial resistance. <sup>c)</sup> Charge-transfer resistance. <sup>d)</sup> The equivalent circuit of the battery during the discharge and charge process.



## Reference

1. L. A. Adams, S. D. Poynton, C. Tamain, R. C. T. Slade and J. R. Varcoe, *ChemSusChem*, 2008, **1**, 79-81.